

This article was downloaded by:

On: 25 January 2011

Access details: *Access Details: Free Access*

Publisher *Taylor & Francis*

Informa Ltd Registered in England and Wales Registered Number: 1072954 Registered office: Mortimer House, 37-41 Mortimer Street, London W1T 3JH, UK



Liquid Crystals

Publication details, including instructions for authors and subscription information:

<http://www.informaworld.com/smpp/title~content=t713926090>

Electro-optical properties of holographically patterned polymer-stabilized cholesteric liquid crystals

Eric R. Beckel^{ab}; Lalgudi V. Natarajan^{bc}; Vincent P. Tondiglia^{bc}; Richard L. Sutherland^{bc}; Timothy J. Bunning^b

^a General Dynamics Information Technology, Dayton, OH 45431 ^b Air Force Research Laboratory, WPAFB, OH 45433 ^c Science Applications International Corporation, Dayton, OH 45431

To cite this Article Beckel, Eric R. , Natarajan, Lalgudi V. , Tondiglia, Vincent P. , Sutherland, Richard L. and Bunning, Timothy J.(2007) 'Electro-optical properties of holographically patterned polymer-stabilized cholesteric liquid crystals', *Liquid Crystals*, 34: 10, 1151 – 1158

To link to this Article: DOI: 10.1080/02678290701663753

URL: <http://dx.doi.org/10.1080/02678290701663753>

PLEASE SCROLL DOWN FOR ARTICLE

Full terms and conditions of use: <http://www.informaworld.com/terms-and-conditions-of-access.pdf>

This article may be used for research, teaching and private study purposes. Any substantial or systematic reproduction, re-distribution, re-selling, loan or sub-licensing, systematic supply or distribution in any form to anyone is expressly forbidden.

The publisher does not give any warranty express or implied or make any representation that the contents will be complete or accurate or up to date. The accuracy of any instructions, formulae and drug doses should be independently verified with primary sources. The publisher shall not be liable for any loss, actions, claims, proceedings, demand or costs or damages whatsoever or howsoever caused arising directly or indirectly in connection with or arising out of the use of this material.

Electro-optical properties of holographically patterned polymer-stabilized cholesteric liquid crystals

ERIC R. BECKEL†§, LALGUDI V. NATARAJAN‡§, VINCENT P. TONDIGLIA‡§,

RICHARD L. SUTHERLAND‡§ and TIMOTHY J. BUNNING*§

†General Dynamics Information Technology, 5100 Springfield Pike, Suite 509, Dayton, OH 45431, USA

‡Science Applications International Corporation, 4031 Colonel Glenn Highway, Dayton, OH 45431, USA

§Air Force Research Laboratory, WPAFB, OH 45433, USA

(Received 10 November 2006; in final form 22 April 2007; accepted 15 May 2007)

Electro-optical properties of cholesteric liquid crystals (LCs) with holographically patterned polymer stabilization were examined. It is hypothesized that increasing the LC domain size in a single dimension, relative to a random three-dimensional network of LC pockets separated by polymer strands, will allow enhanced electro-optical properties of the final device. Prior to holographic patterning, polymer stabilization with large elastic memory was generated by way of high irradiation intensities and optimized material choices. High irradiation intensities are required for the holographic patterning process to maintain polymer layer formation. At optimized conditions, polymer patterning of the stabilization allowed for an approximate 20% increase in the clear state transmission of the device, and allowed for an approximate $3\text{ V}\mu\text{m}^{-1}$ reduction in the overall switching voltage as compared to an analogous floodlit irradiated sample. Switching times were increased at most threefold with holographic patterning, but all relaxation times were below 20 ms. The enhanced electro-optical properties appear to stem from a single dimension domain size increase, which allows for a reduction in the LC/polymer interaction.

1. Introduction

Photonic crystal technologies have undergone extensive research for optical [1, 2] and electro-optical [3–5] applications, including waveguides [6–8], optical filters [9], phase modulators [10] and lasers [11, 12]. Cholesteric liquid crystals (CLCs) are a type of one-dimensional (1D) photonic crystal that demonstrate a photonic band gap. These materials selectively reflect circularly polarized light due to the existence of a macroscopic helical structure, where the wavelength of reflected light is on the order of the helical pitch of the LC [13]. The wavelength of reflected light is given by the following equation:

$$\lambda = n_{\text{ave}}P, \quad (1)$$

where λ is the centre wavelength of the reflection notch, n_{ave} is the average refractive index of the LC determined by $n_{\text{ave}} = (n_o + n_e)/2$ and P is the pitch of the cholesteric helix. n_o and n_e are the ordinary and extraordinary

refractive indices of the LC, respectively. The bandwidth, $\Delta\lambda$, of the spectral reflection is given by:

$$\Delta\lambda = \Delta nP, \quad (2)$$

where $\Delta n = n_e - n_o$ is the birefringence of the LC. Due to the dielectric anisotropy of the LC molecules, the orientational order of these materials can be influenced with the application of an electric field, causing two possible reorientations of the CLC. First, at small applied voltages, the macroscopic helix is broken into domains of smaller helices that are orientated in random directions. This state, called the focal conic state, causes the device to be highly scattering. At larger applied voltages, the LC molecules in the focal conic domains are realigned into a uniform homeotropic alignment, which allows for a clear state of the device. This LC reorientation to the clear state is rapid with the application of a sufficiently large electric field. After the electric field is removed, the return to the cholesteric planar orientation is inhibited due to the long lifetime of the highly scattering focal conic state. To avoid this undesired prolonged focal conic lifetime, a small concentration of monomer can be polymerized into the system, which acts as an elastic memory for the

*Corresponding author. Email: timothy.bunning@wpafb.af.mil

rapid reorientation into the planar aligned cholesteric state.

Polymer stabilization of CLCs typically is classified in one of two distinct fabrication methods, i.e. polymer-stabilized cholesteric textures (PSCTs) [14–21] and polymer-stabilized cholesteric liquid crystals (PSCLCs) [22–30]. In PSCTs, high-functionality monomers are polymerized in the LC to form a highly crosslinked matrix. Due to small polymer domain sizes that impart strong elastic constraint on LC molecules, application of a strong electric field allows only for the reorientation into the focal conic conformation. Thus, if the CLC is formulated such that the reflective notch resides in the infrared spectrum, this device can be switched reversibly between a visible light clear state and a highly scattering state in a rapid fashion. In contrast, PSCLCs use lower functionality monomers that are polymerized in the LC to form a low crosslink density matrix. Due to the larger polymer domain sizes of this network, which reduce the polymer influence on the LC molecules, application of a strong electric field is capable of reorienting the LC molecules into the homeotropic state. Therefore, if the CLC is formulated such that the reflection resides within the visible spectrum, this device can be switched reversibly between a visible light reflective state and a visible light clear state in a rapid fashion. PSCLC systems will encompass the thrust of the research reported here.

Despite the lower crosslink density matrix associated with PSCLCs, there still exists several electro-optical problems with these devices. First, due to the elastic memory of the stabilizing polymer matrix that acts to keep the LC molecules in the cholesteric planar alignment, large applied voltages are required to reach the maximum transmission of the homeotropically aligned clear state. Secondly, at this maximum transmission, substantial scatter can exist due to incomplete reorientation of LCs into the homeotropic alignment [22, 25, 29, 30]. This scattering is most prominent in the violet to blue wavelength regime.

In this paper, we report the potential benefits of holographically patterning the polymer stabilization. A previous attempt at holographic patterning of the polymer stabilization in CLCs attempted to create a Bragg reflection notch within the CLC by use of highly functional mesogenic and non-mesogenic materials [31]. In the work of Date *et al.* [31], a tilted polymeric structure was created within the device, and application of an electric field generated a narrow-notch Bragg reflection due to the refractive index variation of the polymer structure and the reoriented CLC. Due to the high crosslink density of the stabilizing polymer, reorientation of the LC with an applied electric field was not substantial and the original reflection notch of the CLC remained

evident. In this study, we focus on utilizing lower functionality mesogenic monomers patterned in a 1D reflection-type grating geometry, such that reorientation to the homeotropic alignment is facilitated. We theorize that by increasing the LC domain size in a single dimension, relative to an isotropic polymer network, through the periodic polymer patterning process, we can decrease the required voltage for the clear state and increase the amount of homeotropically aligned LCs to increase the overall transmission of the device. This greater realignment should allow for transmission dynamics to be optimized.

2. Experimental

2.1. Materials

Stock CLC was made from a mixture of nematic LC (BL038, EMD Chemicals, Inc, Hawthorne, NY) and chiral dopant (CB15, EMD Chemicals, Inc). Monomers for polymer stabilization were a liquid crystalline diacrylate (RM82, EMD Chemicals, Inc) and a liquid crystalline monoacrylate (RM23, EMD Chemicals, Inc). Photopolymerization was initiated with an ultraviolet photoinitiator (Irgacure 651, Ciba Specialty Chemicals, Tarrytown, NY). All chemicals were used as received.

2.2. Test cell fabrication

Liquid crystal test cells were assembled in-house. ITO-coated glass, with dimensions of 38 mm × 25 mm × 1.1 mm, was used as the cell substrates (Part # CCC410-1, Colorado Concept Coatings LLC, Longmont, CO). A 0.125 wt% solution of Elvamide 8023R (donated by DuPont Engineering Polymers, Wilmington, DE) in methanol was spin-coated onto the ITO glass substrates at a spread speed of 1800 RPM for 6 s and spin speed of 3800 RPM for 45 s to form a polymer alignment layer. Elvamide 8023R is a methanol-soluble nylon that does not require baking prior to cell assembly. The coated substrates were rubbed with a felt cloth to form the alignment layer. Substrates were assembled with an approximate 21 mm overlap with antiparallel alignment. The final test cells were sealed with an ultraviolet photocurable optical adhesive (NOA 81, Norland Products, Cranbury, NJ). Five-micron glass rod spacers (PF-50, Nippon Electric Glass Co., Ltd., Kanzaki, Shiga, Japan) were dispersed in the optical adhesive prior to cell assembly to allow for the desired cell thickness.

2.3. CLC syrup

Approximately 51 wt% BL038 and 49 wt% CB15 were mixed to form the stock CLC, which showed a

reflection notch centred at about 530 nm. To this stock CLC, 10 wt% of RM23 and 1 wt% of Irgacure 651 were added. Crosslinking density studies were explicitly studied by varying the RM82 concentration from 1.5 to 5.2 wt% in the above solution. The solution was mixed with a magnetic stir bar at 55°C for approximately 5 minutes to ensure that the monomers and initiator were completely dissolved within the CLC. The final CLC/monomer syrup was filled into LC test cells via capillary action.

2.4. Holographic patterning

Holographic patterning was accomplished via a single prism set-up [32, 33]. In this set-up, a right-angle prism (CVI Optical Components, Covina, CA) was placed in the beam path from an Ar⁺ laser (Innova Sabre 10, Coherent, Inc, Santa Clara, CA) with the laser set to 363.8 nm wavelength. Laser intensity on the sample was 60 mW cm⁻² and total irradiation time was 90 s. The prism was oriented such that the laser beam is perpendicular to the square face of the right angle prism, while the sample to be patterned was placed on the hypotenuse of the prism. Index matching fluid ($n=1.52$, Cargille Laboratories, Inc, Cedar Grove, NJ) was used between the prism and the front glass substrate of the sample to allow light to couple into the sample, and reduce Fresnel reflections and optical cross-talk during irradiation. The incoming laser beam enters the sample and is totally internally reflected from the rear glass substrate. The reflected beam interferes with the incident beam forming an interference pattern within the sample. This interference pattern causes areas of high light intensity and low light intensity to be generated within the cell, allowing for the formation of the patterned polymer structure. Figure 1 shows an idealized cartoon of the subsequent structure. Polymer layers are generated in x-y plane of the substrate and

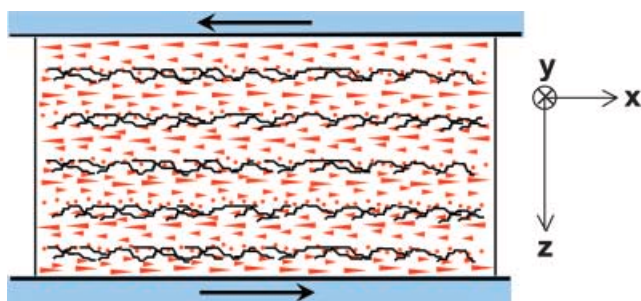


Figure 1. Side view of idealistic holographically patterned CLC. Polymer layers are formed in the x-y plane. The bilayer spacing is approximately 160 nm.

the bilayer spacing was calculated to be approximately 160 nm from the Bragg equation:

$$\Lambda = \lambda_w / 2n_{ave} \sin \theta, \quad (3)$$

where Λ is the bilayer spacing, λ_w is the writing beam wavelength (363.8 nm), n_{ave} is the average refractive index (~ 1.60) and θ_B is the angle of incidence of the writing beam and the polymer planes (45°).

2.5. Device testing

Transmission spectra were analysed with a miniature fibre optic spectrometer (SQ2000, Ocean Optics, Inc, Dunedin, FL). Light was supplied from a fibre optic illuminator (Fiber-Lite PL-800, Dolan-Jenner Industries, Lawrence, MA) that emitted broadband white light from a 150 W halogen bulb. A 1 kHz square wave ac voltage was supplied by a function generator (33120A, Agilent Technologies, Palo Alto, CA) connected to a high voltage amplifier (Mound Technical Solutions, Inc, Miamisburg, OH). The maximum voltage applied to the cells was 130 V_{rms}. Applied voltages above this maximum exceeded the dielectric breakdown of the LC material and caused catastrophic failure of the sample.

3. Results

The formulation of most PSCLC devices requires the use of monoacrylate monomers in combination with small amounts of diacrylate monomers to develop the low crosslink density matrix required to allow for homeotropic realignment with an applied electric field. In the polymerization process of these systems, low light intensity and long irradiation times are typically utilized to develop a polymer network with sufficient elastic memory for the fast relaxation into the cholesteric planar alignment [22, 25–27]. When the incident irradiation intensity is increased for the polymerization process, the termination rate is subsequently increased, causing shorter polymer kinetic chain lengths to be developed. The stabilization potential of these shorter polymer kinetic chain lengths is negatively impacted and the relaxation time to the planar cholesteric state is greatly increased. However, in holographic patterning processes, high light intensity irradiation is required to ensure proper layer formation without significant inter-layer cross polymerization. A method to avoid the limited stabilization caused by high light intensity irradiation was to increase the crosslinking agent, which facilitates the network development and limits the low molecular weight chain formation. To demonstrate that high irradiation intensities can be utilized to create sufficient stabilization, a sample with a moderate

concentration of diacrylate crosslinker was subjected to high intensity floodlit irradiation. This proof of concept analysis is the basis for subsequent holographically patterned samples via high light intensity irradiation. Figure 2 shows the transmission spectrum and switching dynamics of this proof of concept floodlit PSCLC sample with 3.6 wt% diacrylate irradiated with 60 mW cm^{-2} intensity.

As can be seen from figure 2 b, the relaxation time to switch from the clear state to the cholesteric planar state is approximately 1 ms. This rapid return speed demonstrates that the polymer matrix formed during the high intensity irradiation is capable of stabilizing the CLC. Moreover, figure 2 a further validates the strong elastic memory strength of the formed polymer matrix. At the maximum voltage of 130 V, the device exhibits moderate scattering, indicating that polymer is acting to keep the LC molecules in the planar alignment and significantly retarding the reorientation to the homeotropic alignment. In contrast, CLC systems without polymer stabilization show extremely prolonged relaxation times, which are on the order of minutes to hours to return to the planar alignment. The return to the planar alignment of these unstabilized systems is compounded by a long-lived local energy minimum of the focal conic state. In stabilized systems, this local energy minimum is bypassed, and the system rapidly relaxes into the planar alignment.

The previous results demonstrate that high irradiation intensities are capable of forming a polymer matrix with ample elastic memory to stabilize the CLC planar structure. Before electro-optical analyses can be performed on holographically patterned samples, it must be discerned that the patterning process does not adversely affect the CLC order, and thus alter the reflective properties of the system. Figure 3 compares

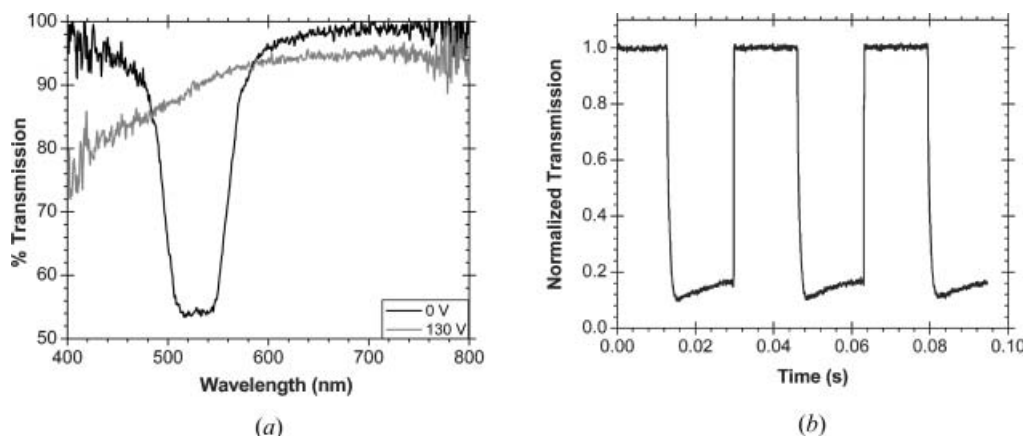


Figure 2. (a) Transmission spectra of floodlit irradiated sample. Application of threshold voltage (grey line) shows significant clear state scatter. (b) Switching dynamics of floodlit sample. Rise time is approximately $400 \mu\text{s}$ and fall time is approximately 1 ms, determined by a 90%:10% analysis. Probe beam wavelength was 543 nm . $I_0 = 60 \text{ mW cm}^{-2}$, $[\text{XL}] = 3.6 \text{ wt\%}$, $T = 5 \mu\text{m}$.

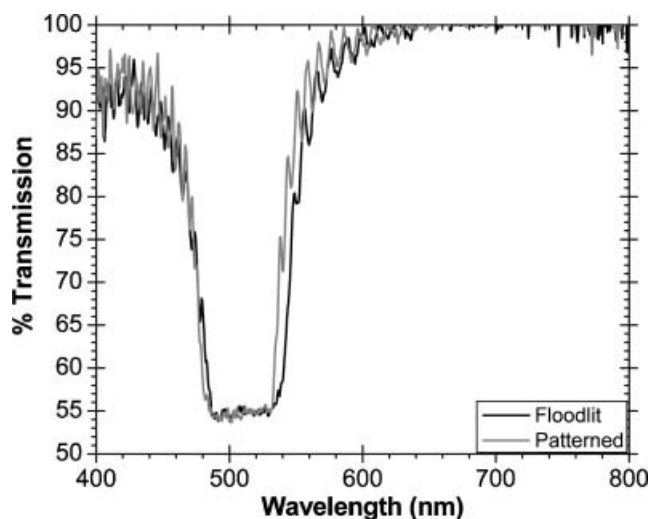


Figure 3. Reflection notch appearance post-polymerization. Patterning of polymer stabilization (grey line) does not adversely affect notch appearance. $I_0 = 60 \text{ mW cm}^{-2}$, $[\text{XL}] = 3.6 \text{ wt\%}$, $T = 5 \mu\text{m}$.

the post-polymerization notch characteristics of both floodlit and patterned devices that were irradiated with 60 mW cm^{-2} intensity.

It is evident that the holographic process does not distort or alter the CLC order during the polymerization process. There is minimal difference between the floodlit and patterned samples in the appearance of the reflection notch. Moreover, there is minimal notch broadening in both cases, as shown by the correlation between the theoretical and experimental reflection bandwidth. Equation (2) predicts that the breadth should be approximately 76 nm ($n_{\text{ave}} \cong 1.61$, $\lambda \cong 530 \text{ nm}$, $\Delta n \cong 0.23$), whereas the actual measured full width half maximum breadth is 75 nm .

Patterning of the polymer stabilization increases the domain size in a single dimension (z-dimension) as compared to a floodlit device. This increased domain size was hypothesized to decrease the polymer/LC interaction and increase the transmission of the system. Figure 4 shows the transmission spectrum and switching dynamics of a patterned sample as compared to an analogous floodlit sample. Each sample contains 3.6 wt% diacrylate crosslinker and was irradiated with 60 mW cm^{-2} intensity.

Figure 4a illustrates that there is a significant increase in the transmission of the patterned sample over the floodlit sample at the maximum voltage of 130 V. The switched patterned sample achieved approximately 90% transmission at $\lambda=400 \text{ nm}$, whereas the switched floodlit sample only achieved approximately 70% at this same wavelength. As hypothesized, the increase domain size in the z-dimension has decreased the polymer/LC interaction in the patterned sample and has allowed for a greater amount of the LC molecules to reorient into the homeotropic alignment. This greater realignment has decreased the scattering centres, and increased the overall transmission of the device. This decreased polymer/LC interaction is further illustrated in figure 4b, where the relaxation time for the clear to reflective state is increased slightly to 3 ms, as opposed to the 1 ms for the floodlit sample, as shown in figure 2b. This increased relaxation time is due to the increased domain size in the z-dimension, which reduces surface-to-volume ratio of the LC to the polymer. This reduced surface-to-volume ratio causes the LC molecules to be influenced to a lower extent than in the floodlit device, and the relaxation time to the planar orientation is increased. However, the 3 ms relaxation

time is still well within the required speeds for display applications.

A further important property of these systems is the switching voltage response, such as the voltages for the onset of switching and the voltage needed to reach the plateau transmission of the system. The voltage for the onset of switching gives greater detail into the overall polymer/LC interaction, as lower voltages indicate reduced interactions. The switching voltage responses for the patterned and floodlit samples are given in figure 5. Responses for $\lambda=440 \text{ nm}$, outside the reflection notch, and $\lambda=530 \text{ nm}$, inside the reflection notch, are shown as a function of increased voltage.

In figure 5, there are three distinct zones associated with the reorientation of the LC molecules. First, at low voltages, the molecules remain in the planar orientation and the transmission remains constant. When the voltage exceeds a critical value, the molecules are capable of overcoming the elastic memory of the polymer and reorient into the focal conic conformation. This reorientation is signified by a decrease in the transmission as the focal conic domains form and scatter the incident light. Increasing the voltage increases the focal conic domain formation until the transmission reaches a minimum. This minimum transmission signifies the maximum focal conic domain concentration, and a further voltage increase will start to reorient these domains into the homeotropic conformation. This reorientation into the homeotropic allows for the increase in transmission that is evident beyond this maximum focal conic domain concentration. At large voltages, the LC molecules have reached a maximum reorientation and the transmission plateaus to a constant value. Thus, the two important voltages to analyse are the voltage for the

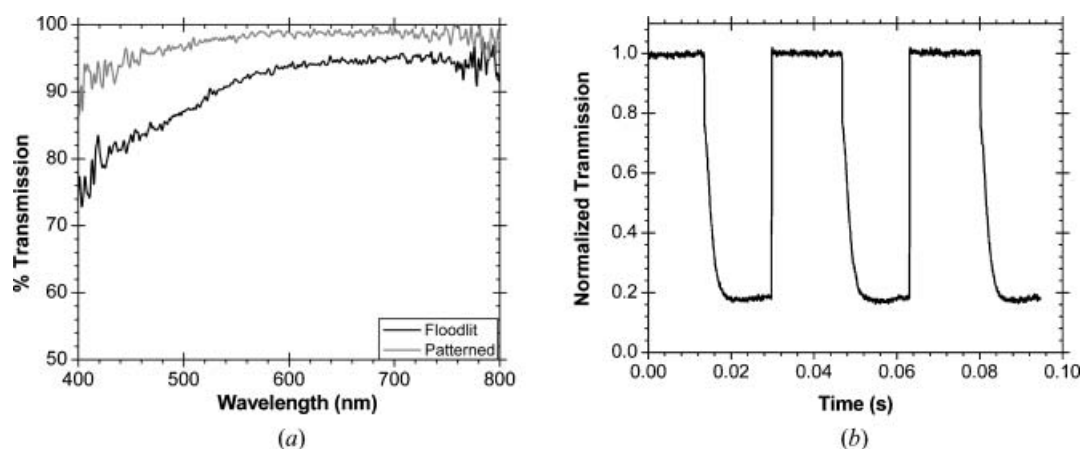


Figure 4. (a) Transmission spectra of floodlit irradiated (black line) and patterned devices (grey line). Patterned device shows significant clear state scatter improvement over floodlit device. (b) Switching dynamics of patterned device. Rise time is approximately $500 \mu\text{s}$ and fall time is approximately 3 ms, determined by a 90%:10% analysis. Probe beam wavelength was 543 nm . $I_0=60 \text{ mW cm}^{-2}$, $[\text{XL}]=3.6 \text{ wt } \%$, $T=5 \mu\text{m}$.

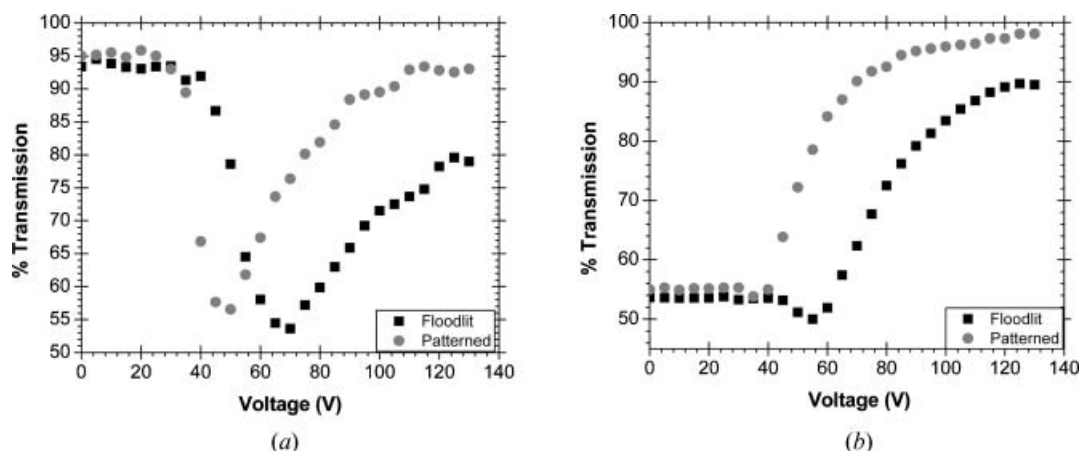


Figure 5. Switching voltage response. (a) Outside reflection notch ($\lambda=440$ nm) and (b) inside reflection notch ($\lambda=530$ nm) are shown. Patterned devices (grey circles) show a reduction in the ultimate voltage required for maximum transmission. $I_0=60$ mW cm $^{-2}$, [XL]=3.6 wt %, $T=5$ μ m.

onset of the focal conic reorientation (low voltage) and the voltage for the maximum realignment (high voltage). From figures 5 a and 5 b, it can be seen that the patterned sample shows lower voltages for both the onset of focal conic reorientation and maximum homeotropic realignment as opposed to the floodlit sample. For the patterned sample, the voltage for initial reorientation is approximately 25 V, and the voltage for the maximum transmission is approximately 110 V. For the floodlit sample, the voltage for the initial reorientation is approximately 40 V and the voltage for the maximum transmission is approximately 125 V. Therefore, there is an approximate 3 V μ m $^{-1}$ reduction in the required switching voltage by utilizing the patterned device. This switching voltage reduction is due to the lower polymer/LC surface-to-volume ratio of the patterned sample, which leads to a reduced polymer influence on the LC molecules.

The 3.6 wt % diacrylate crosslinker results have shown that by holographically patterning these samples, enhanced electro-optical properties can be achieved. By altering the diacrylate crosslinker concentration, the polymer domain size can be varied. Increasing the diacrylate concentration will decrease the polymer domain size, while decreasing the diacrylate concentration will increase the domain size. Changing the domain size of the polymer stabilization will have a profound effect on the overall switching dynamics of the devices, both floodlit and patterned. Figure 6 illustrates the diacrylate concentration effect on the transmission characteristics of the samples. The y-axis of this figure is the transmission difference between the patterned and floodlit samples:

$$\Delta T = T_p - T_f, \quad (4)$$

where T_p is the transmission of the patterned cell and T_f is the transmission of the floodlit cell, analysed at $\lambda=500$ nm

and 130 V applied voltage. A ΔT of zero indicates that the patterned cell and the floodlit cell have equivalent transmissions.

Figure 6 shows three regions of stabilization, which are understabilized, stabilized, and overstabilized. The understabilized region is for diacrylate concentrations of approximately 2.6 wt % and below, whereas the overstabilized region is for diacrylate concentrations of approximately 4.7 wt % and above. In the understabilized regions, the low diacrylate concentration creates a low crosslink density polymer, which allows for the formation of large domain sizes throughout the sample. These large domains limit the polymer/LC interaction, which limits the stabilization of the system. Since the patterned samples and floodlit samples in the

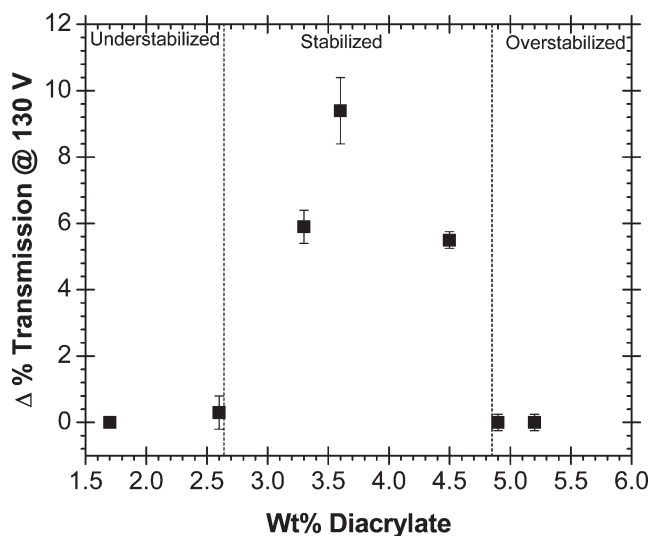


Figure 6. Transmission difference between patterned and floodlit devices analysed at $\lambda=500$ nm.

understabilized regime show similar switching dynamics, it is hypothesized that the domain sizes in the floodlit sample are similar or larger than the bilayer spacing of the polymer layers in the patterned sample. Thus, by patterning the polymer stabilizer, there probably is not a significant increase in the domain size in any single dimension, which would account for the similar switching dynamics. In the overstabilized regions, the higher diacrylate concentration creates a higher crosslink density polymer, which creates much smaller domain sizes throughout the sample. These domain sizes increase the polymer/LC interaction and act to keep more of the LC molecules in the planar alignment. Moreover, the increased diacrylate concentration will additionally have a profound effect on the patterned samples, since the increased crosslinking sites will allow for a greater chance of inter-layer cross-polymerization. This interlayer cross-polymerization will limit the effectiveness of patterning process due to the reduction in the domain size in the z-dimension.

Figure 7 demonstrates the strong elastic memory of the overstabilized regime, as both the patterned sample and floodlit sample still retain a portion of the original reflection notch with 130 V applied voltage. In the overstabilized patterned sample, there is a slight increase in the transmission as compared to the floodlit sample, indicating a slight increase in the z-dimension domain size of the patterned sample. However, the retention of the original reflection notch indicates strong polymer/LC interactions, most probably due to small domain sizes in all dimensions. In the stabilized

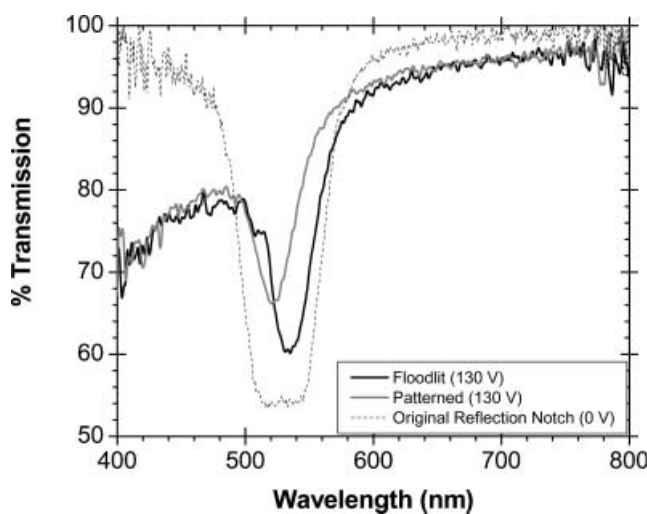


Figure 7. Transmission spectra of floodlit irradiated (black line) and patterned devices (grey line) with an applied voltage of 130 V. Original reflection notch without an applied voltage is shown (black dotted line). Overstabilization evident due to partial retention of reflection notch at threshold voltage. $I_0 = 60 \text{ mW cm}^{-2}$, $[XL] = 5.2 \text{ wt} \%$, $T = 5 \mu\text{m}$.

region, in which diacrylate concentrations are approximately between 2.6 wt% and 4.7 wt%, there is significant difference in the transmission of the patterned samples and the floodlit samples. This transmission difference stems from the increase in the domain size in the z-dimension, as discussed earlier.

Relaxation times for each set of diacrylate concentrations can be evaluated for a qualitative analysis of the polymer/LC interaction. Figure 8 shows the relaxation times for floodlit and patterned samples with varying concentrations of diacrylate.

As stated above, diacrylate concentrations of approximately 2.6 wt% and below were considered understabilized. The relaxation times for these samples further indicate this understabilization, as both the floodlit and patterned samples showed times of approximately 20 ms, which is approximately one order of magnitude longer than the stabilized samples. Additionally, due to the large domain sizes within these understabilized samples, the return speeds for the floodlit and patterned samples are similar. Samples with diacrylate concentrations of approximately 4.7 wt% and above were considered overstabilized. The relaxation times additionally support this overstabilization, as both the floodlit and patterned samples with 5.2 wt% diacrylate showed times of 100 μs , which is approximately one order of magnitude faster than the stabilized samples. Finally, in the stabilized region, all patterned samples demonstrated relaxation times that were slightly slower than the counterpart floodlit samples. This longer relaxation time is further evidence of increased domain size in the z-dimension for the patterned samples. This increased domain size in

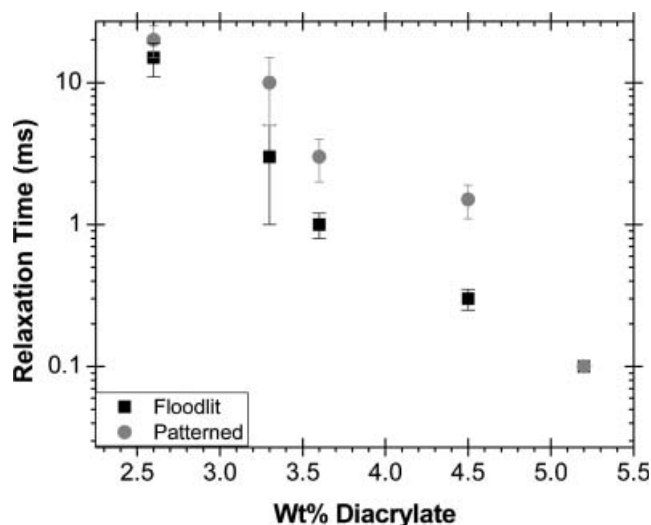


Figure 8. Switching dynamics of diacrylate concentration study. Relaxation time indicates time to return to reflective state from clear state when electric field is removed.

the z-dimension slightly decreases the overall elastic memory of the stabilizing polymer structure, thus increasing the relaxation times.

Direct evidence of domain size and layer thickness by morphological analysis could not be accomplished for the aforementioned samples. The high LC content of the samples maintains a highly fluid system that does not allow for sample sectioning for microscopy without highly specialized techniques. However, a layered polymer structure was evidenced through Bragg reflection experiments. By offsetting the polymer layer structure from the layer normal, the Bragg reflection could be separated from the Fresnel reflection. This offsetting was accomplished by placing a 10° wedge on the back of the sample during holographic polymerization. The 10° wedge should give a 5° tilt of the polymer layer structure. Reflection analysis of a sample with 4 wt% LC diacrylate gave a bilayer spacing of approximately 160 nm, a layer tilt of approximately 5°, and a diffraction efficiency of 0.04%. The low diffraction efficiency is due to the low refractive index modulation between the polymer-rich layers and the LC-rich layers in the aligned state. The bilayer spacing and layer tilt analysis agree strongly with the theoretical calculations and strongly support existence of periodic polymer layers.

4. Conclusions

Electro-optical properties of holographically patterned polymer-stabilized cholesteric liquid crystals were analysed. Stabilization utilizing high irradiation intensities was first demonstrated, as this high intensity is required for holographic patterning. Stabilization via moderate amounts of diacrylate crosslinker allowed for enhanced electro-optical properties. Switching voltages were reduced by approximately $3\text{ V}\mu\text{m}^{-1}$ and clear state transmission was increased by approximately 20% in the blue part of the visible spectrum. These enhancements were due to the increased domain size in a single dimension, which is a consequence of the patterning process.

Acknowledgements

The authors of this paper would like to acknowledge AFOSR/NL, the Strategic Partnership for Research in Nanotechnology (SPRING), and AFRL for the support of this project.

References

- [1] W. Park, C.J. Summers. *Appl. Phys. Lett.*, **84**, 2013 (2004).
- [2] W. Park, C.J. Summers. *Opt. Lett.*, **27**, 1397 (2002).
- [3] S.P. Gorkhali, J. Qi, G.P. Crawford. *J. opt. Soc. Am. B*, **23**, 149 (2006).
- [4] G. Alagappan, X.W. Sun, P. Shum, M.B. Yu, M.T. Doan. *J. Opt. Soc. Am. B*, **23**, 159 (2006).
- [5] M. Schmidt, M. Eich, U. Huebner, R. Boucher. *Appl. Phys. Lett.*, **87**, 121110 (2005).
- [6] A. Säynäjoki, M. Mulot, S. Arpiainen, J. Ahopelto, H. Lipsanen. *J. Opt. A*, **8**, S502 (2006).
- [7] M. Notomi, A. Shinya, S. Mitsugi, E. Kuramochi, H.-Y. Ryu. *Opt. Exp.*, **12**, 1551 (2004).
- [8] S.J. McNab, N. Moll, Y.A. Vlasov. *Opt. Exp.*, **11**, 2927 (2003).
- [9] I. Del Villar, I.R. Matias, F.J. Arregui, R.O. Claus. *Opt. Exp.*, **11**, 430 (2003).
- [10] I. Abdulhalim. *J. Opt. A*, **2**, L9 (2000).
- [11] H. Altug, D. Englund, J. Vučković. *Nature Phys.*, **2**, 484 (2006).
- [12] H. Yu, B.Y. Tang, J. Li, L. Li. *Opt. Exp.*, **13**, 7243 (2005).
- [13] P.G. de Gennes. In *The Physics of Liquid Crystals*, W. Marshall, D.H. Wilkinson (Eds), pp. pp.219–276, Clarendon Press, Oxford (1974).
- [14] Y.-H. Lin, H. Ren, Y.-H. Fan, Y.-H. Wu, S.-T. Wu. *J. appl. Phys.*, **98**, 043112 (2005).
- [15] C.-Y. Huang, K.-Y. Fu, K.-Y. Lo, M.-S. Tsai. *Opt. Exp.*, **11**, 560 (2003).
- [16] H. Ren, S.-T. Wu. *J. appl. Phys.*, **92**, 797 (2002).
- [17] H. Guillard, P. Sixou. *Mol. Cryst. liq. Cryst.*, **364**, 647 (2001).
- [18] I. Dierking, L.L. Kosbar, A.C. Lowe, G.A. Held. *Liq. Cryst.*, **24**, 387 (1998).
- [19] I. Dierking, L.L. Kosbar, A.C. Lowe, G.A. Held. *Liq. Cryst.*, **24**, 397 (1998).
- [20] D.-K. Yang, J.L. West, L.-C. Chien, J.W. Doane. *J. appl. Phys.*, **76**, 1331 (1994).
- [21] D.-K. Yang, L.-C. Chien, J.W. Doane. *Appl. Phys. Lett.*, **60**, 3102 (1992).
- [22] M. Mitov, E. Nouvet, N. Dessaud. *Eur. Phys. J. E*, **15**, 413 (2004).
- [23] Y.J. Kwon, W.J. Lee, S.H. Paek, I. Kim, K. Song. *Mol. Cryst. liq. Cryst.*, **377**, 325 (2002).
- [24] V. Laus, F. Roussel, J.-M. Buisine. *Ferroelectrics*, **277**, 75 (2002).
- [25] C. Binet, M. Mitov, M. Mauzac. *J. appl. Phys.*, **90**, 1730 (2001).
- [26] H. Guillard, P. Sixou, L. Reboul, A. Perichaud. *Polymer*, **42**, 9753 (2001).
- [27] A. Lavernhe, M. Mitov, C. Binet, C. Bourgerette. *Liq. Cryst.*, **28**, 803 (2001).
- [28] U. Theissen, S.J. Zilker, T. Pfeuffer, P. Strohhriegel. *Adv. Mater.*, **12**, 1698 (2000).
- [29] R.A.M. Hikmet, H. Kemperman. *Liq. Cryst.*, **26**, 1645 (1999).
- [30] R.A.M. Hikmet, H. Kemperman. *Nature*, **392**, 476 (1998).
- [31] M. Date, T. Hisaki, Y. Takedchi. *Mol. Cryst. liq. Cryst.*, **368**, 53 (2001).
- [32] L.V. Natarajan, C. Shepherd, D. Brandelik, S. Chandra, R.L. Sutherland, T.J. Bunning, V.P. Tondiglia, D. Tomlin. *Chem. Mater.*, **15**, 2477 (2003).
- [33] L.V. Natarajan, D.P. Brown, J. Wofford, V.P. Tondiglia, R.L. Sutherland, P.F. Lloyd, T.J. Bunning. *Polymer*, **47**, 4411 (2006).